Naval Research Laboratory

Washington, DC 20375-5320

NRL/MR/6110--11-9369

Numerical Simulations of Pressure Spikes within a Cylindrical Launch Tube due to a Bursting Helium Flask

HAROLD D. LADOUCEUR
BENJAMIN GOULD

Chemical Dynamics and Diagnostics Branch
Chemistry Division

November 9, 2011

REPORT DOCUMENTATION PAGE

Form Approved
OMB No. 0704-0188

1. REPORT DATE *(DD-MM-YYYY)*	**2. REPORT TYPE**	**3. DATES COVERED** *(From - To)*
09-11-2011	Memorandum	April 2010 – August 2011

4. TITLE AND SUBTITLE

Numerical Simulations of Pressure Spikes within a Cylindrical Launch Tube due to a Bursting Helium Flask

5a. CONTRACT NUMBER

5b. GRANT NUMBER

5c. PROGRAM ELEMENT NUMBER
0603826D8Z

6. AUTHOR(S)

Harold D. Ladouceur and Benjamin Gould

5d. PROJECT NUMBER

5e. TASK NUMBER

5f. WORK UNIT NUMBER

7. PERFORMING ORGANIZATION NAME(S) AND ADDRESS(ES)

Naval Research Laboratory, Code 6110
4555 Overlook Avenue, SW
Washington, DC 20375-5320

8. PERFORMING ORGANIZATION REPORT NUMBER

NRL/MR/6110--11-9369

9. SPONSORING / MONITORING AGENCY NAME(S) AND ADDRESS(ES)

Under Secretary of Defense
(Acquisition, Technology and Logistics)
3010 Defense Pentagon
Washington, DC 20301-3010

10. SPONSOR / MONITOR'S ACRONYM(S)

11. SPONSOR / MONITOR'S REPORT NUMBER(S)

12. DISTRIBUTION / AVAILABILITY STATEMENT

Approved for public release; distribution is unlimited.

13. SUPPLEMENTARY NOTES

14. ABSTRACT

A numerical model to simulate the bursting of a high-pressure flask of helium gas located within a cylindrical launch tube is described. The model provides an upper estimate for the launch tube wall pressures by assuming that the helium flask failure can be treated as a bursting balloon. The gas dynamic equations for the expansion of the 5000 psig helium region are solved utilizing the finite element program FlexPDE to obtain time-dependent solutions for pressure, gas density, and velocity. The work is motivated by a desire to understand and interpret field tests conducted by NRL at Blossom Point in June 2010, for the experimental fuel cell (XFC) unmanned aerial system (UAS). The primary objective of these tests was to determine the failure mode of the hydrogen fuel flask and the extent of fragmentation damage. The test demonstrated that the fragmentation damage to the XFC launcher tube was minimal. Launch tube side wall and end cap pressure–time measurements were also recorded during the flasks burst for both helium and hydrogen gases. This transducer data is compared with the numerical simulations of the gas dynamic model.

15. SUBJECT TERMS

Experimental fuel cell (XFC)	Bursting helium flask
Hydrogen fuel cell	Numerical simulation of pressure burst
Pressure vessel explosion	Unmanned aerial system (UAS)

16. SECURITY CLASSIFICATION OF:			**17. LIMITATION OF ABSTRACT**	**18. NUMBER OF PAGES**	**19a. NAME OF RESPONSIBLE PERSON**
a. REPORT	**b. ABSTRACT**	**c. THIS PAGE**			Harold D. Ladouceur
Unclassified	Unclassified	Unclassified	UU	16	**19b. TELEPHONE NUMBER** *(include area code)* (202) 767-3558

Standard Form 298 (Rev. 8-98)
Prescribed by ANSI Std. Z39.18

CONTENTS

EXECUTIVE SUMMARY

A numerical model to simulate the bursting of a high-pressure flask of helium gas located within a cylindrical launch tube is described. The model provides an upper estimate for the launch tube wall pressures by assuming that the helium flask failure can be treated as a bursting balloon. The gas dynamic equations for the expansion of the 5000 psig helium region are solved utilizing the finite element program FlexPDE to obtain time-dependent solutions for pressure, gas density and velocity. The work is motivated by a desire to understand and interpret field tests conducted by NRL at Blossom Point in June, 2010 for the experimental fuel cell (XFC) unmanned aerial system (UAS). The primary objective of these tests was to determine the failure mode of the hydrogen fuel flask and the extent of fragmentation damage. The test demonstrated that the fragmentation damage to the XFC launcher tube was minimal. Launch tube side wall and end cap pressure-time measurements were also recorded during the flasks burst for both helium and hydrogen gases. Transducer data are compared with the numerical simulations of the gas dynamic model.

Numerical Simulations of Pressure Spikes within a Cylindrical Launch Tube due to a Bursting Helium Flask

BACKGROUND[1]

The Naval Research Laboratory (NRL) is exploring the use of polymer electrolyte membrane (PEM) fuel cells and gaseous hydrogen to power unmanned air vehicles. One area of safety concern is the failure of the fuel tank (H_2 flask) which contains 5000 psig hydrogen. For use aboard naval vessels, containment of this highly flammable gas inside the launching system, which is a cylindrical pressure vessel, is of paramount importance. The hydrogen flasks are manufactured for the NRL Experimental Fuel Cell (XFC) program by HyperComp Engineering, Inc. The flasks are made of a composite carbon fiber overwrapped aluminum liner and are available in two sizes of 1.9 L or 4.0 L volume (Fig. 1). The 1.9 L flask has a hydrostatic bursting pressure greater than 9925 psig and the 4.0 L flask has a hydrostatic burst pressure greater than 8850 psig. The 1.9 L flask is cylindrical in shape with an approximate length of 10 inches and a diameter of 3.8 inches.

Figure 1 Four 1.9 L and a 4.0 L hydrogen flasks.

In June of 2010 these pressurized flasks were destructively tested at Blossom Point inside an open section of the XFC launch tube. The primary test objective was to obtain information on the methods of failure when the pressurized flasks were subjected to mechanical damage. The

Manuscript approved August 24, 2011.

damage was created by firing an aluminum slug with a conical tip (.024 lb) from a pneumatic air gun used in NAVSEA 8020.8B friability tests. The nature of the flask failure depended upon the impact point of the gun's slug. End bell failures resulted in pinhole leaks with subsequent rocketing of the flask inside the launch tube. Induced side-wall failures caused the flasks to burst.

The flasks were mounted inside an opened section of the XFC launch tube (Fig. 2). The launch tube is approximately 20 inches in diameter and 36 inches long. In actual deployment, the closed launch vessel would be filled with nitrogen gas to eliminate the possibility of hydrogen combustion.

Figure 2 Image of XFC launch tube with 1.9 L flask inside. Pressure transducers location are indicated by A, B, and C.

Pressure transducers were located in the launch tube side wall (A,B), and the end cap. The side-wall and end-cap transducers were Kistler 601B1s blast probes. These probes are utilized to measure pressure in blast experiments and have response times less than 4 μs and a pressure range of 0-1000 psi.

PRESSURE EXPANSION MODEL

The sudden release of the high pressure gas contained within the fuel flask can be modeled as a gas jet flowing out of a given diameter circular hole (end-bell failure) or by assuming that the flask walls burst like a balloon (side-wall failure). In the side-wall failure mode, the initial conditions that specify the gas pressure and density correspond to a cylindrical region without confining walls whose volume and location within the XFC launch tube are identical to the fuel flask geometry. However, this representation of the initial conditions can introduce numerical problems due to the sharp spatial and temporal discontinuities at the flask wall boundary. Thus, a smooth and continuous analytic function (super Gaussian) of position whose volume integral yields the flask volume is utilized to describe the initial conditions of pressure and density. In the model developed here, the initial helium pressure distribution is given by

$$P(r,z) = (P_{He} - P_{N_2}) \exp\left(-2\left(\frac{r}{r_c} \right)^8 \right) \exp\left(-2\left(\frac{z - z_0}{(z_2 - z_1).66} \right)^{10} \right) + P_{N_2},$$

where P_{He} denotes the initial helium tank pressure, P_{N_2} is the nitrogen pressure within the XFC launch tube, and r_c corresponds to the helium flask radius (4.83 cm). The bottom and top planes of the cylindrical helium flask intersect the z-axis at z_1 and z_2 respectively. The parameter z_0 is given by

$$z_0 \equiv \left(\frac{z_2 + z_1}{2} \right).$$

Thus, the flask center is located on the z-axis at z_0. The exponents are empirically selected to provide an initial pressure region which corresponds to the fuel flask geometry. The number .66 is determined by the requirement that the volume integral over the initial high-pressure region equals 1.9 L. Some numerical simulations were run with larger values of the exponents. The numerical results were not very sensitive to the values of the exponents. Figure 3 shows a contour plot of the initial pressure distribution within the launch tube calculated from the analytic model.

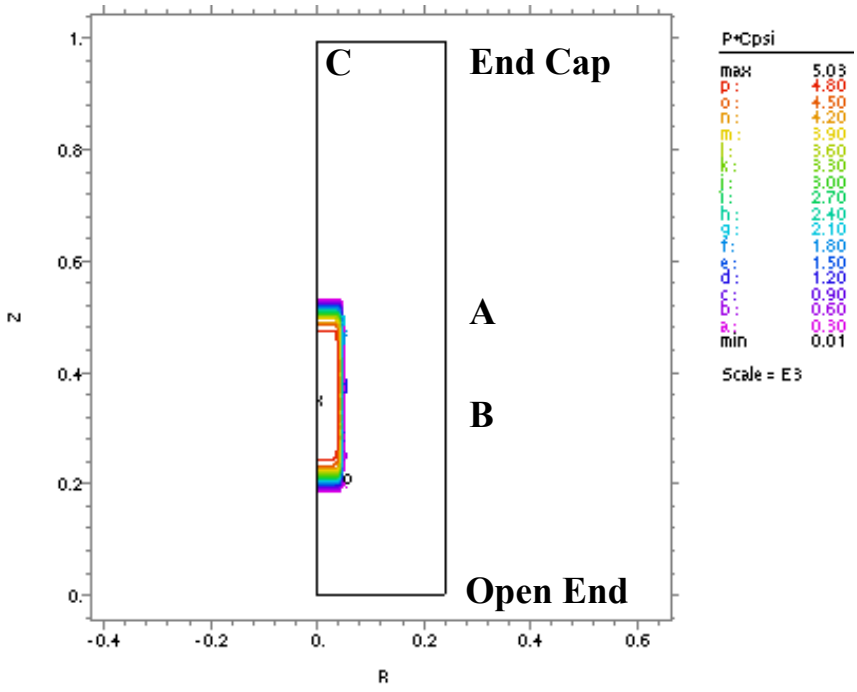

Figure 3 Initial pressure contours (psi) within the cylindrical launch tube. Pressure probe positions are indicated by A, B, and C.

The system of partial differential equations (PDEs) which govern the expansion of the high-pressure helium gas is given by [2]

$$\frac{\partial \rho}{\partial t} + \nabla \cdot \left(\rho \vec{V} \right) = 0$$

$$\rho \left(\frac{\partial \vec{V}}{\partial t} + \vec{V} \cdot \nabla \vec{V} \right) + \nabla P = 0$$

$$\frac{\partial P}{\partial t} + \vec{V} \cdot \nabla P - a^2 \left(\frac{\partial \rho}{\partial t} + \vec{V} \cdot \nabla \rho \right) = \frac{\partial P}{\partial t} + \vec{V} \cdot \nabla P + \gamma P \nabla \cdot \vec{V} = 0 \qquad a^2 = \gamma R_G T$$

The first equation represents the conservation of total mass, the second equation is the Euler momentum equation and the last equation is the speed of sound equation which can be employed in place of the energy equation for an isentropic expansion. The variables of interest are the gas density ρ, the pressure P within the launch tube, and the gas velocity $\vec{V}$. The quantity a is the

speed of sound which depends upon the gas temperature T. γ is the specific heat ratio of the gas (1.66 He) and R_g is the specific gas constant (2078.6 J/kg-K).

The system of PDEs given above governs the flow of an ideal or inviscid fluid. In developing numerical solutions of such time-dependent systems, small inaccuracies introduced at the boundaries or in the initial conditions may cause the calculations to become unstable[3]. If the fluid is physically viscous, these instabilities would be damped or dissipated by the introduction of a viscosity term. However, the viscosity of most gases is quite small and the damping effect requires a fine grid resolution and rather small time steps to resolve shock structures. Practical numerical implementation of actual gas viscosity effects can be directly incorporated into thin regions (boundary layers) near physical surfaces. For the bulk fluid flow, such implementation is computationally expensive. An alternative approach first proposed by Von Neumann and Richtmeyer[4] is to introduce an artificial viscosity to resolve shock structure. Artificial viscosity provides a mathematical dissipation analogous to the real physical viscosity of the gas. The calculation of the jump conditions developed across a shock structure is obtained by spreading the shock structure over several grid points or a "smear distance" ΔL. This approach provides the correct jump conditions, but bears no relation to the actual shock thickness produced by physical viscosity. The introduction of artificial viscosity terms, gives the following system of equations

$$\frac{\partial \rho}{\partial t} + \nabla \cdot \left(\rho \vec{V} \right) = \varepsilon \nabla^2 \rho$$

$$\frac{\partial \vec{V}}{\partial t} + \vec{V} \cdot \nabla \vec{V} + \frac{\nabla P}{\rho} = \varepsilon \nabla \cdot \left(\nabla \vec{V} \right)$$

$$\frac{\partial P}{\partial t} + \vec{V} \cdot \nabla P - a^2 \left(\frac{\partial \rho}{\partial t} + \vec{V} \cdot \nabla \rho \right) = \frac{\partial P}{\partial t} + \vec{V} \cdot \nabla P + \gamma P \nabla \cdot \vec{V} = \varepsilon \nabla^2 P$$

$$\varepsilon \equiv a \Delta L \qquad a^2 \equiv \gamma R_G T$$

The quantity ε has the dimension of length^2/time similar to the Fick's law diffusion coefficient. The introduction of this term into the equations provides for spatial diffusion of the dependent variables over time. The insertion of the artificial viscosity term into the PDEs may seem somewhat *ad hoc*. However, one can rationalize this approach by considering a modification of the textbook derivation of the conservation laws. In the customary derivation, the PDEs are derived from Taylor series expansions of the dependent variables over a small spatial control volume with neglect of the quadratic terms in $\Delta x, \Delta y, \Delta z$. The retention of these quadratic terms will provide the artificial viscosity formulation.

NUMERICAL RESULTS

Figure 4 shows the calculated pressure at the launch tube side wall for a probe located at position A in Figure 3 (.242 m, .6 m) as a function of time. The calculated pressure history at the wall is quite sensitive to the probe's axial position. Figure 5 shows the calculated pressure at the launch tube wall for a probe located at position B (.242 m, .359 m) in Figure 3. This position corresponds to a location which is centered on the lateral surface of the fuel flask.

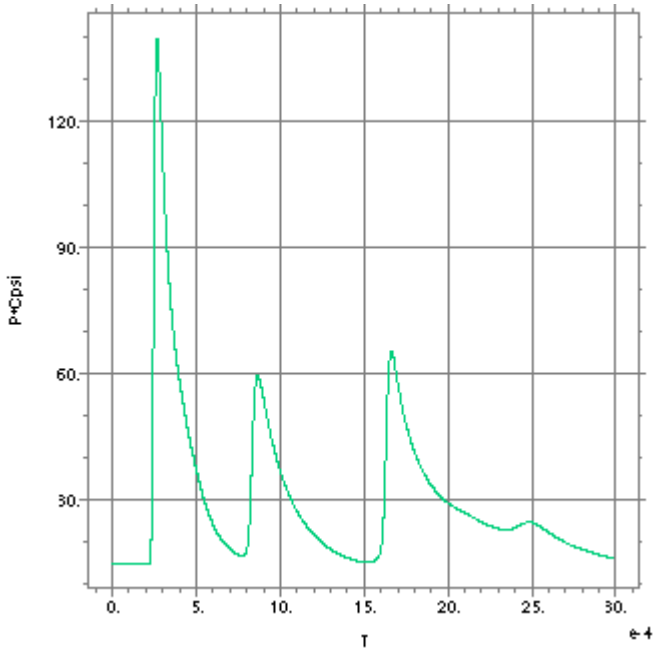

Figure 4 Calculated side wall pressure (psi) for a probe located at position A in Figure 3. The initial conditions correspond to Figure 3.

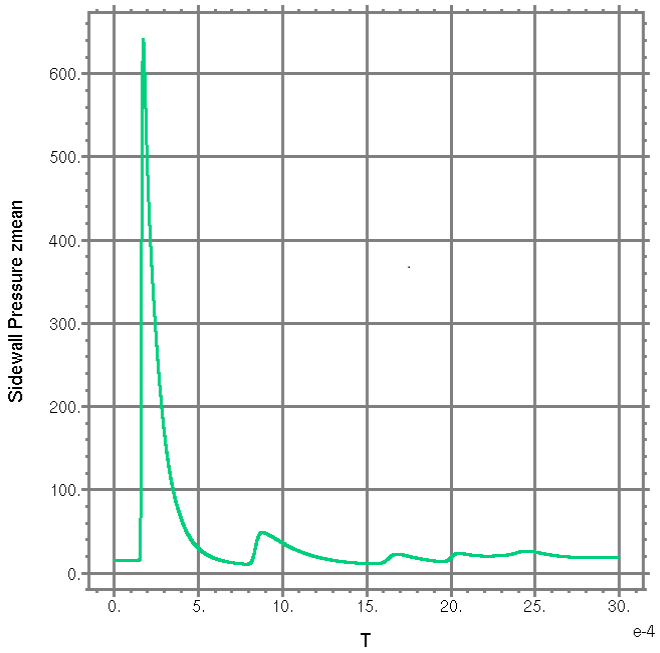

Figure 5 Calculated side wall pressure (psi) for a probe located at position B in Figure 3. The initial conditions correspond to Figure 3.

The side wall pressure varies with the axial location by as much as factors or five to six. The pressure amplitude also is dependent upon the assumed initial pressure. To account for the difference in peak pressures, the initial flask pressure in the numerical simulations prior to bursting was reduced to allow for the gas's mechanical energy (Helmholtz energy A(T,V)) loss in tearing the flask apart. The Helmholtz energy is defined by[5]

$$A \equiv E - TS \qquad dA = -PdV - SdT$$

where E denotes the internal energy and S is the entropy. In an isothermal expansion $dT = 0$, and the Helmholtz energy change is equivalent to the negative of the reversible pressure-volume work w_{rev}. If one assumes *ideal gas law* behavior and an isothermal process, the change in the Helmholtz energy with pressure can be calculated from the following equation

$$\Delta A = P_1 V_1 \ln\left(\frac{P_2}{P_1}\right) = R_g T \ln\left(\frac{P_2}{P_1}\right) = -w_{rev}$$

where P_1 is the initial gas pressure, V_1 denotes the initial flask volume and T is the initial gas temperature. Figure 6 shows the calculated change of the Helmholtz energy with pressure. The black curve assumes an isothermal expansion and ideal gas behavior. The reference state is taken as $P_2 = 1.0\,atm$ pressure and a temperature $T = 300K$. Above 50 atm pressure, the system deviates from ideal gas law behavior as shown by the red curve. This curve was obtained using the Cheetah 6.0 equation of state for Helium[6] and calculating $P_1V_1 - P_2V_2$ directly from the

Cheetah output. Note, that the Cheetah code utilizes the ideal gas law to calculate ΔA as indicated by the black dots in Figure 6. A key point of this figure is the nonlinear behavior of the Helmholtz energy as a function of pressure. At 5000 psi (340 atm), the available Helmholtz energy is 872 cal/g. A 50% reduction in the available energy corresponds to an initial pressure of about 254 psi (

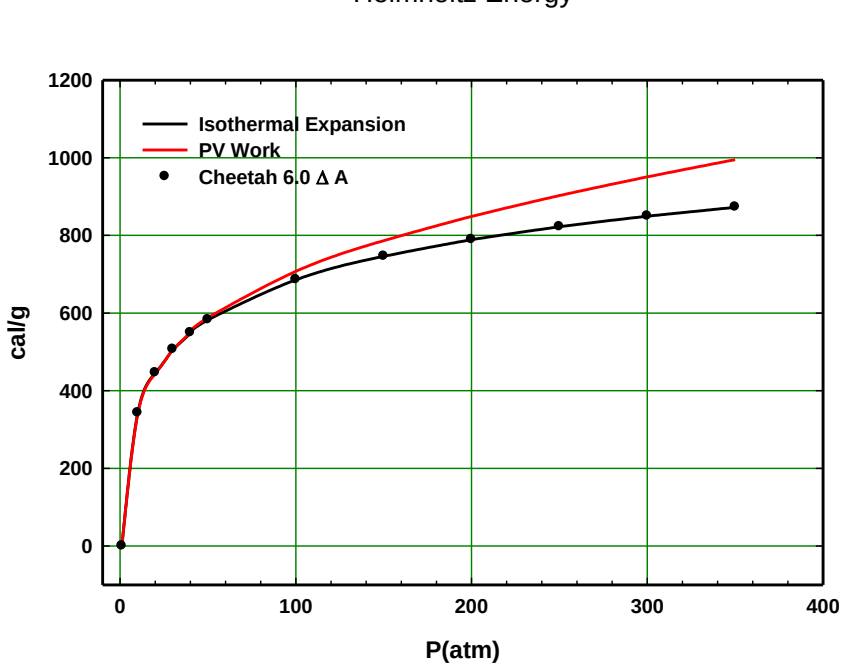

Figure 6 Calculated Helmholtz energy as a function of flask pressure. The PV curve is a calculation for non-ideal gas behavior.

To account for the difference in the observed peak pressure versus the model prediction, a number of simulations were run with reduced initial flask pressures. This is justified because the walls of the flask do not simply dissolve and for the energetics of a pressure vessel failure, the theoretical stored mechanical energy is often derated[7].

Of particular interest is the pressure dynamics on the end cap (position C) because in the XFC-UAS launch canister the end cap is the structurally weakest member and most prone to failure during a flask burst. Figure 7 compares the calculated pressure at the end cap to the measured pressure during a flask burst. Qualitatively, the model shows similar behavior to the experimental data with a high initial peak followed by damped pressure oscillations in time. The peak intervals occur at similar timescales and show reasonable agreement between the experiment and model given the disparity between the balloon bursting model and the observed flask failure behavior. Peak pressures are somewhat higher in the model, which assumes perfectly rigid launch tube walls unlike the real system; this assumption might contribute to the difference in peak pressure since it provides no mechanism for absorption of the incident energy in the pressure pulse.

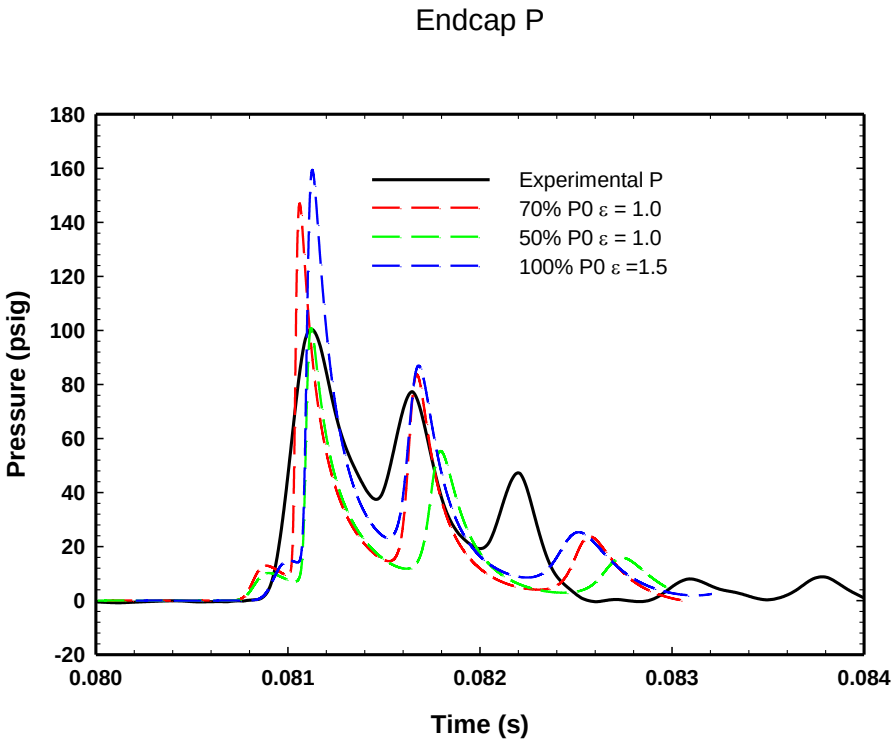

Figure 7 Experimental and calculated end cap pressures as a function of time for probe located at position C in Figure 3.

END-BELL FAILURE MODE LEAKAGE RATE

The rate of gas leakage from the fuel flask due to a circular puncture of radius r_h can be calculated by assuming that the gas flow is choked, isentropic and a quasi-steady process. The assumption that the gas expansion is quasi-steady is justified by the observation that the instantaneous gas pressure throughout the initial expansion process is considerably higher than the initial pressure within the launch tube and that the pressure relaxation time with an acoustic speed of $a = 2634 m/s$ over the flask length is on the order of 0.1 ms. The mass flow (kg/s) is given by[8]

$$\frac{dM}{dt} = \frac{\Gamma \pi r_h^2 P(t)}{\sqrt{\gamma R_g T}} \qquad \Gamma \equiv \gamma \left(\frac{2}{\gamma + 1} \right)^{\frac{(\gamma+1)}{2(\gamma-1)}} \qquad \Gamma = .81,$$

where $\gamma = 1.4$ for a diatomic gas and $P(t)$ is the instantaneous fuel flask pressure. At 5000 psi, the initial mass flow rate for hydrogen through a 2 mm radius hole is 0.134 kg/s. By use of the ideal gas law, the mass flow rate can be integrated to give an explicit expression for the fuel flask pressure $P(t)$ as a function of time

In tl

is V_c

and

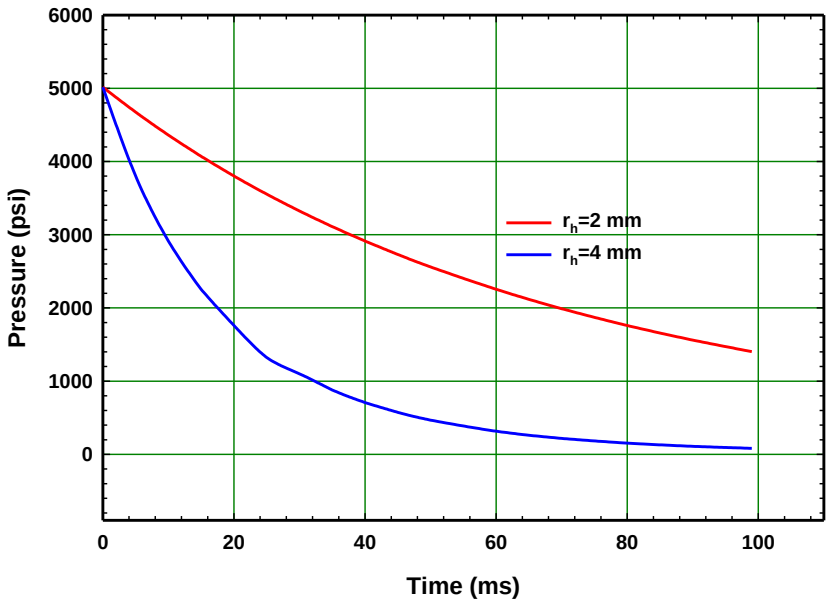

Figure 8 Hydrogen flask pressure as a function of time due to hole in end bell.

A crude estimate of the initial thrust developed in the end failure mode can be determined from[9]

$$F = C_F A_h P(t).$$

F denotes the thrust (Newton or pound), A_h is the area of the hole and C_F is the thrust coefficient. In an actual rocket nozzle, the thrust coefficient determines the amplification of the thrust due to gas expansion in the supersonic portion of the nozzle as compared to the thrust developed if the chamber pressure acted over the throat area only. Since we have assumed choked flow through the hole and there is no supersonic nozzle, the thrust coefficient is 1. For a hole with a radius of 4 mm and an initial pressure of 5000 psi, the thrust is 1.73 kN or 390 lbf.

CONCLUSION

The numerical model and the experimental pressure dynamics show reasonable agreement given the simplicity of the failure model (bursting balloon) and the complexity of the actual failure. The calculated peak pressures are quite sensitive to the specified initial conditions and probe location. The actual fuel vessel pressure immediately after bursting is reduced due to the work done by the confined gas upon rupturing the vessel walls. The assumption of an isothermal expansion is consistent with the experimental observation that the final gas temperature is near ambient temperature and provides an upper limit for the explosion energy. Calculations assuming an isentropic gas expansion provide a lower limit on the available explosion energy due to adiabatic cooling. The effective pressure just after vessel rupture can be determined from the Helmholtz free energy (Fig. 6) provided one knows the work done in rupturing the vessel walls. As shown in Figure 6, this reduction in pressure due to rupture work is nonlinear.

The use of artificial viscosity in solving the gas dynamic equations provides a simple and direct algorithm which was quickly implemented in the FlexPDE 6 finite-element code. A preliminary sensitivity analysis (Fig. 7) revealed a weak dependence of peak pressure upon the choice of ε. Of greater concern in the accuracy of the model prediction is the determination of the correct initial conditions. The formulated model is nonlinear and sensitive to the specified initial conditions. Future work could include a more realistic model of the fuel flask failure and allow for pressure-time (impulse) interactions with mechanical deformation on the launch tube walls. The present model assumes a rigid cylindrical tube which is opened at one end. A closed system with hydrogen gas could be explored. Due to acoustic speed differences and hydrogen's diatomic gas properties, the predictions would differ.

Some preliminary calculations have been undertaken with Comsol 4.2. This is a finite-element code which can incorporate multi-physics. A geometry identical to the one developed here has been constructed with both a Gaussian-like pressure profile and an actual flask with wall containing a circular cut. The Comsol code can incorporate super-sonic flow, heat and mass transfer and the elastic response and deformation of various material components within the model.

AKNOWLEDGEMENTS

The authors would like to thank the Office of Naval Research and the Office of the Secretary of Defense (OSD) Office of Technology Transition and the OSD Rapid Reaction Technology Office for financial support on this research.

REFERENCES

1. "The Fragmentation Damage Caused by a H_2 Flask Burst on the XFC Launch Tube," NRL Letter Report, Ser 6110/232, December 7, 2010.
2. Zucrow, M.J. and Hoffman, J. D., "Gas Dynamics", John Wiley & Sons, New York, NY (1976), Volume 1 p 548.
3. Anderson, John, D., Jr,"Modern Compressible Flow with Historical Perspective," McGraw-Hill, New York, NY (1982), pp 327-330.
4. Von Neumann, J. and R. D. Richtmyer, "A Method for the Numerical Calculation of Hydrodynamic Shocks," J. Appl. Phys., Vol. 21, No. 3, pp 232-237 (1950).
5. Smith, J.M. and H. C. Van Ness, "Introduction to Chemical Engineering Thermodynamics," 3rd edition, McGraw-Hill, New York, NY (1975), pp 169-172, 66-72.
6. Cheetah 6.0, Lawrence Livermore National Laboratory, Revision 1794 (2010).
7. Crowl, Daniel, A.," Calculating the energy of explosion using thermodynamic availability," J. Loss Prev. Process Ind., Vol. 5, No. 2, pp 109-118 (1992); See also Appendix B of electronic resource by the same author "Understanding Explosions," ISBN 1591246288 (2003).
8. Demetriades, S.T., "On the Decompression of a Punctured Pressure Cabin in Vacuum Flight," *Jet Propulsion*, Vol. 24, No. 1, pp 35-36 (1954).
9. Sutton, G.P., "Rocket Propulsion Elements, An Introduction to the Engineering of Rockets," 6th edition, John Wiley & Sons, New York, NY (1992), pp 58-59.